Human Molecular Genetics, 2014, Vol. 23, No. 23 **6163–6176**
doi:10.1093/hmg/ddu337
Advance Access published on July 1, 2014

Epigenetic remodelling and dysregulation of *DLGAP4* is linked with early-onset cerebellar ataxia

Sheroy Minocherhomji[1,2,†], Claus Hansen[1,2], Hyung-Goo Kim[3,‡], Yuan Mang[1,2], Mads Bak[1,2], Per Guldberg[4], Nickolas Papadopoulos[5], Hans Eiberg[2], Gerald Dayebga Doh[2], Kjeld Møllgård[2], Jens Michael Hertz[6], Jørgen E. Nielsen[7,8], Hans-Hilger Ropers[3], Zeynep Tümer[1,9], Niels Tommerup[1,2], Vera M. Kalscheuer[3] and Asli Silahtaroglu[1,2,*]

[1]Wilhelm Johannsen Centre for Functional Genome Research, [2]Department of Cellular and Molecular Medicine, Faculty of Health Sciences, University of Copenhagen, Copenhagen N DK-2200, Denmark, [3]Department of Human Molecular Genetics, Max Planck Institute for Molecular Genetics, Berlin 14195, Germany, [4]Danish Cancer Society, Institute of Cancer Biology, Copenhagen DK-2100, Denmark, [5]Ludwig Center for Cancer Genetics, Johns Hopkins Kimmel Cancer Center, Baltimore, MD 21231, USA, [6]Department of Clinical Genetics, Odense University Hospital, Odense C DK-5000, Denmark, [7]Section for Neurogenetics, Department of Cellular and Molecular Medicine, University of Copenhagen, Copenhagen N 2200, Denmark, [8]Danish Dementia Research Centre, Neurogenetics Clinic, Department of Neurology, Rigshospitalet, Copenhagen University Hospital, Copenhagen Ø 2100, Denmark and [9]Applied Human Molecular Genetics, Kennedy Center, Copenhagen University Hospital, Rigshospitalet, Glostrup DK-2600, Denmark

Received April 3, 2014; Revised and Accepted June 26, 2014

Genome instability, epigenetic remodelling and structural chromosomal rearrangements are hallmarks of cancer. However, the coordinated epigenetic effects of constitutional chromosomal rearrangements that disrupt genes associated with congenital neurodevelopmental diseases are poorly understood. To understand the genetic–epigenetic interplay at breakpoints of chromosomal translocations disrupting CG-rich loci, we quantified epigenetic modifications at *DLGAP4* (*SAPAP4),* a key post-synaptic density 95 (PSD95) associated gene, truncated by the chromosome translocation t(8;20)(p12;q11.23), co-segregating with cerebellar ataxia in a five-generation family. We report significant epigenetic remodelling of the *DLGAP4* locus triggered by the t(8;20)(p12;q11.23) translocation and leading to dysregulation of *DLGAP4* expression in affected carriers. Disruption of *DLGAP4* results in monoallelic hypermethylation of the truncated *DLGAP4* promoter CpG island. This induced hypermethylation is maintained in somatic cells of carriers across several generations in a t(8;20) dependent-manner however, is erased in the germ cells of the translocation carriers. Subsequently, chromatin remodelling of the locus-perturbed monoallelic expression of *DLGAP4* mRNAs and non-coding RNAs in haploid cells having the translocation. Our results provide new mechanistic insight into the way a balanced chromosomal rearrangement associated with a neurodevelopmental disorder perturbs allele-specific epigenetic mechanisms at breakpoints leading to the deregulation of the truncated locus.

*To whom correspondence should be addressed at: Centre for Functional Genome Research, Department of Cellular and Molecular Medicine, Faculty of Health Sciences, University of Copenhagen, DK-2200 Copenhagen N, Denmark. Tel: +45 35327621; Fax: +45 35327845; Email: asli@sund.ku.dk
†Present address: Nordea Center for Healthy Aging, Department of Cellular and Molecular Medicine, University of Copenhagen, 2200 Copenhagen N, Denmark.
‡Present address: Department of Obstetrics and Gynecology, Georgia Regents University, Augusta, GA 30912, USA.

INTRODUCTION

The expression of genes are tightly controlled by complex epigenetic mechanisms, including DNA methylation and histone modifications, which are often regulated by *cis* or *trans* acting non-coding RNAs (ncRNAs) (1). Characterizing these epigenetic mechanisms at specific genomic loci remains pivotal in understanding their roles in regulating genome activity (2–4).

Structural variations within the human genome, including balanced chromosomal rearrangements that disrupt genes, are an established cause of human disorders (5). These rearrangements have been used extensively to identify novel disease-causing genes (6,7). They may also serve as natural models to investigate epigenetic mechanisms, as exemplified by translocations that disrupt X-inactivation (8,9) and imprinted gene loci (10), which are mediated by factors acting in *cis* or *trans* (11–13). However, inherited chromosomal rearrangements that induce epigenetic effects associated with neurodevelopmental movement disorders have not been identified. To investigate the allele-specific genetic, epigenetic and gene expression changes mediated by such disease-associated chromosomal rearrangements, we studied the regulatory mechanisms perturbed by a familial chromosomal translocation, t(8;20)(p12;q11.23) associated with early-onset cerebellar ataxia in a large family (6). Our study provides novel insight into the genetic–epigenetic interplay occurring at breakpoints of a disease-associated chromosomal translocation disrupting a CpG island within the human genome.

RESULTS

Characterization of the t(8;20)(p12;q11.23) translocation

The t(8;20)(p12;q11.23) translocation is inherited from both paternal and maternal lineages and co-segregates with full penetrance in all 14 carriers with autosomal dominant early-onset, non-progressive, mild cerebellar ataxia across five generations (6) (Fig. 1A–C). The patients presented with variable phenotypes including gait, ataxia, mild chorea, clumsiness, impaired hand-coordination and tremors, representing the phenotypic plasticity in this neurological disorder (6).

A high LOD score of $Z = 5.12$ ($\theta = 0.0$) indicated a strong linkage between the translocation and the disease. We initially mapped the breakpoints to sequence level by cloning and Southern blot analysis and amplified the breakpoints using genomic DNA obtained from the indexed patient (carrier III.2) and her sister (carrier III.7) together with allele-specific PCR primers listed in Supplementary Material, Table S1 (Fig. 1D and data not shown). We identified a breakpoint on the long (q) arm of chromosome 20 (chr20) at 20q11.23 that disrupted the *DLGAP4* gene [SAP90/PSD-95 associated protein 4 or discs, large (Drosophila) homolog-associated protein 4; *SAPAP-4*], distal to a previously unsequenced gap, which we have subsequently sequenced (14). Although there is limited information in the literature about *DLGAP4*, it is known to be part of a family of five proteins (DLGAP 1–5) that are highly expressed in the rat brain (15) and act as chaperone proteins assisting in the proper recruitment of the postsynaptic density 95 (PSD95) complex. They function in the signalling complex at the postsynaptic density, linking the glutamate receptor binding proteins and the cytoskeleton (16). The chromosome 20 breakpoint of the translocation truncated a CpG island 820 bp downstream of the first un-translated exon of *DLGAP4* isoform a (Fig. 1D and E). The 8p12 breakpoint disrupted a gene-empty region (~107 kb in size) comprising long interspersed nuclear elements and long terminal repeats (Fig. 1D and F).

t(8;20) triggers monoallelic DNA hypermethylation of the disrupted *DLGAP4* CpG island

We investigated whether this rearrangement that truncated a CpG island might have induced an effect on DNA methylation (5-methylcytosine: 5-mC) or DNA hydroxymethylation (5-hydroxymethylcytosine: 5-hmC). Initially, we measured genome-wide DNA hypermethylation and hypomethylation by high-throughput MBD-Seq and MRE-Seq in genomic DNA from peripheral blood lymphocytes (PBLs; somatic cells) of two translocation carrier sisters, III.2 and III.7, and four phenotypically normal, unrelated male and female controls (Controls 1–4). We found no significant changes in DNA methylation patterns; neither on a genome-wide level (Fig. 2A and B) nor on either of the disrupted chromosomes (Supplementary Material, Fig. S1A and B), when compared with control genomes tested here and in all other control human tissues tested elsewhere (17). In strong contrast however, the disrupted *DLGAP4* CpG island was differentially methylated in the two tested translocation carriers (Fig. 2C and D). All controls tested here (Fig. 2C and D) and published elsewhere remained completely hypomethylated at the same locus (17).

To determine the allele-specific DNA methylation status of the normal and disrupted *DLGAP4* CpG islands and the mode of transmission of this epigenetic change in multiple generations of carriers, we performed bisulfite allelic sequencing using DNA from the somatic (PBLs and buccal epithelium) cells of eight translocation carriers, III.2, III.7, IV.1, IV.2, IV.4, IV.9, V.1 and V.7 comprising both males and females, across three generations of the family (Fig. 1A). Additionally, we tested two phenotypically normal family members (IV.6 and V.6) to determine whether they had inherited the DNA methylation change at *DLGAP4* irrespective of carrying the t(8;20)translocation.

Strikingly, transcription factor binding sites (TFBS) within the CpGs juxtaposed to the breakpoint on derivative chromosome 8 (der8) were identified to be hypermethylated in the somatic cells of all eight tested patients (Fig. 2E). In contrast, the undisrupted *DLGAP4* promoter on normal chr20 remained completely hypomethylated in all carriers tested (Fig. 2F). Additionally, the *DLGAP4* promoter remained biallelically hypomethylated (Figs 1D and 2F) in phenotypically normal family members, IV.6 and V.6 with normal karyotypes, and in unrelated normal controls (Controls 1 and 2). These findings confirmed that monoallelic hypermethylation at the disrupted *DLGAP4* CpG island is dependent on t(8;20) translocation and is transmitted across multiple generations of the family. Indeed, we observed a transmission of this epigenetic change at the disrupted *DLGAP4* CpG island from the assessed carrier mothers (III.2 and III.7) with cerebellar ataxia to all their translocation carrier male and female offspring (IV.1, IV.2, IV.4 and IV.9) who were also affected with the disease. This pattern of inheritance was also maintained and transmitted from a carrier father (IV.2) to his offspring (V.1) with the ataxia phenotype.

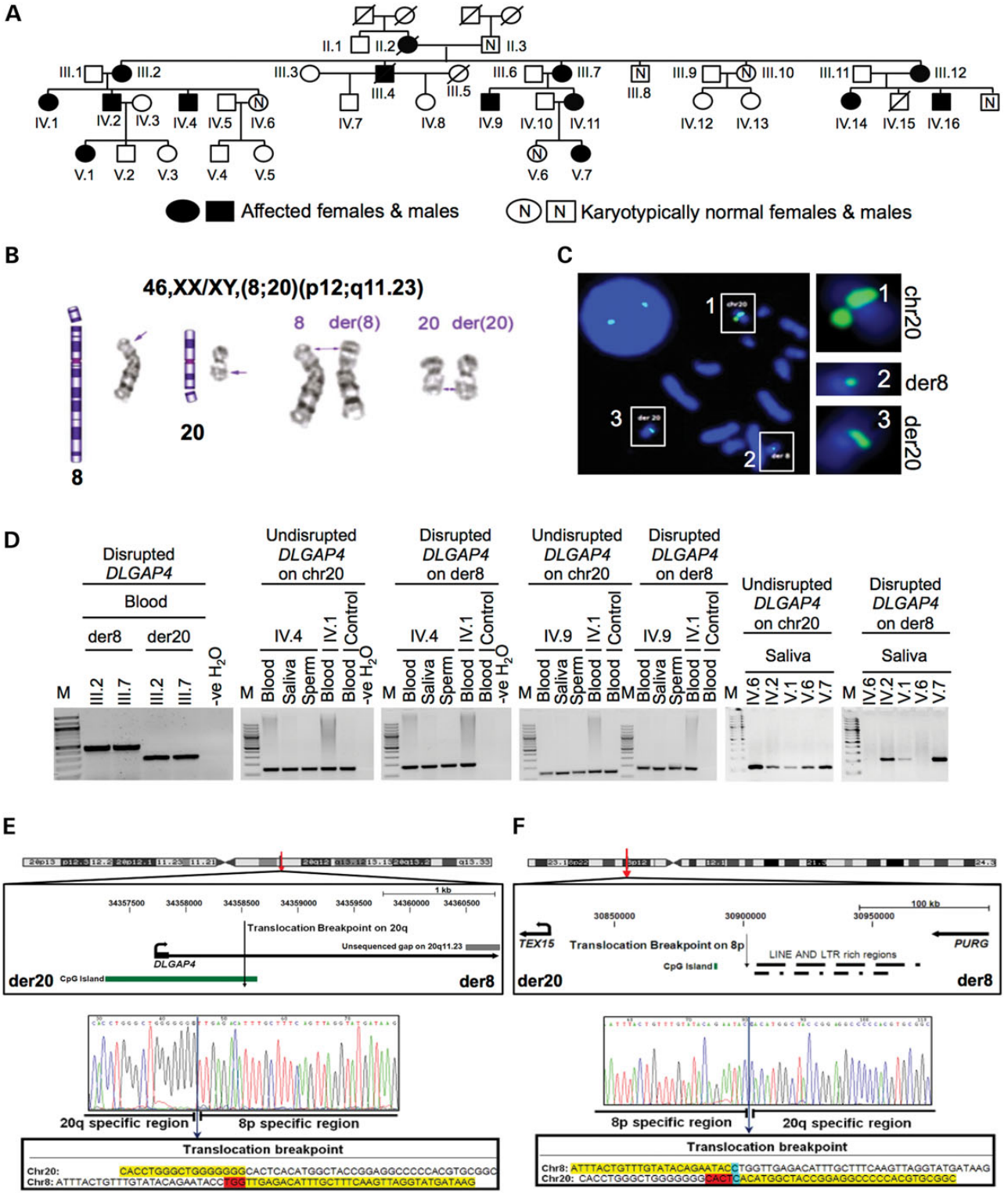

Figure 1. *DLGAP4* is disrupted by the translocation t(8;20)(p12;q11.23) segregating with early-onset, non-progressive, mild cerebellar ataxia. (**A**) Pedigree of investigated family. (**B**) Ideograms and translocation chromosomes. (**C**) *FISH* mapping of chr20q11.23 breakpoint showing three signals using spanning BAC CTD-2301L1. (**D**) PCR amplification of disrupted and undisrupted *DLGAP4* alleles in t(8;20) carriers and phenotypically normal unrelated (controls) or related (IV.6 and V.6) controls. (**E**) Representative UCSC genome browser view of the breakpoint region on 20q11.23 showing disruption of *DLGAP4*, 820 bp downstream (at chr20: 34358534, hg18) of the first untranslated exon. Electropherogram shows base level resolution of the breakpoint on chromosome der20 with a 'TGG' deletion (red highlight). (**F**) Translocation breakpoint on 8p12 (at chr8: 30901056, hg18) disrupts a region dense in repetitive elements. Electropherogram shows the der8 breakpoint region having a 'CACT' deletion (red highlight). The cytosine base (blue highlight) at the breakpoint could be part of 8p or 20q. Yellow highlights indicate the sequence adjacent to breakpoints. Illustrations are drawn to scale; curved arrows denote promoter regions of genes.

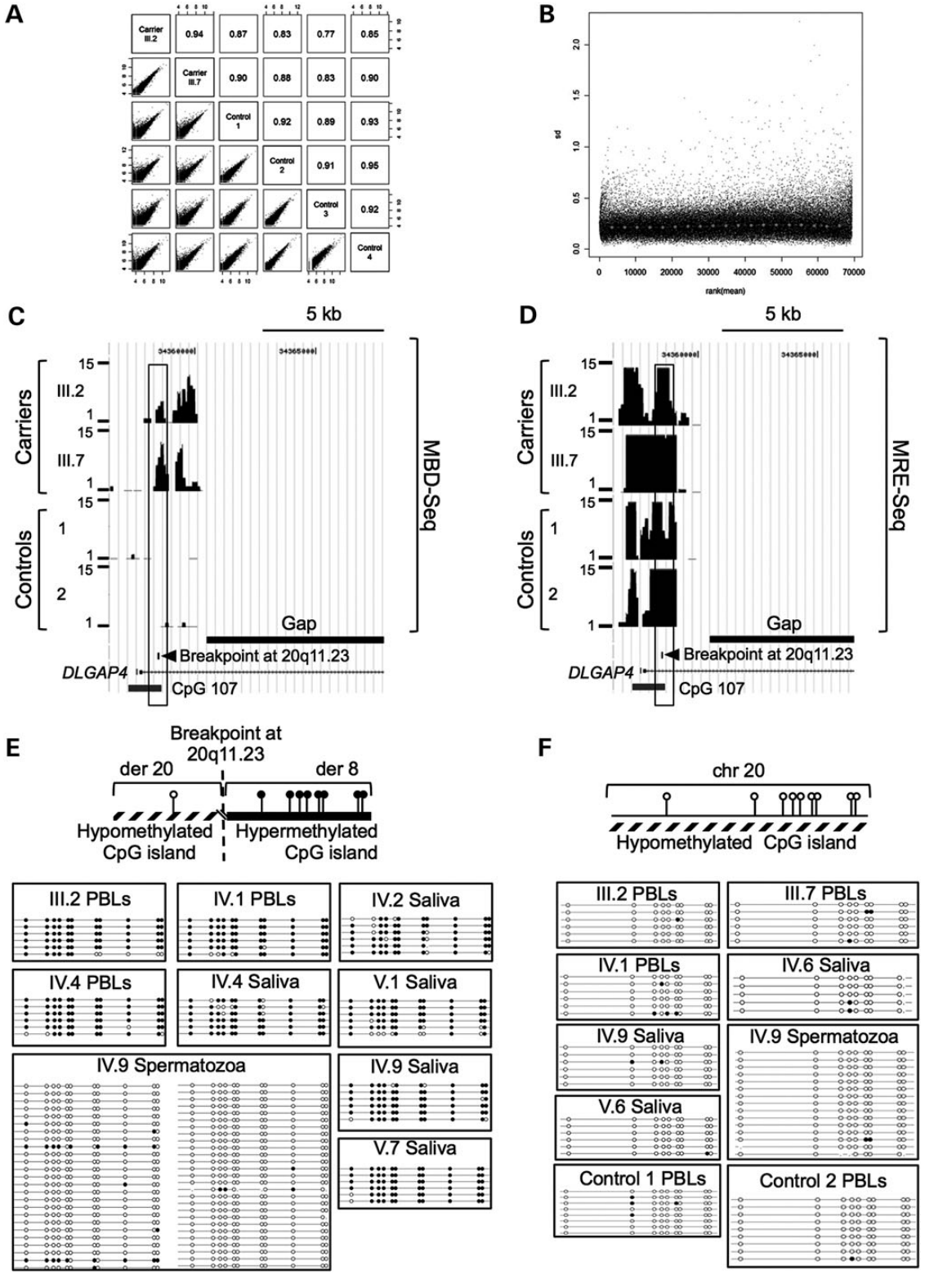

Figure 2. Monoallelic changes in DNA methylation at *DLGAP4* are induced by the t(8;20) translocation. (**A** and **B**) Normalized unique MBD-Seq peak reads in carriers (III.2, III.7) and four normal unrelated controls (Controls 1–4) showing genome-wide distribution of reads and peaks. (**C** and **D**) UCSC genome browser views showing the translocated *DLGAP4* CpG island (CpG 107) to be differentially methylated (hypermethylated: MBD-Seq and hypomethylated: MRE-Seq) in carriers and completely hypomethylated in controls. Rectangles show regions used for bisulfite allelic sequencing (see below). (**E**) Bisulfite allelic sequencing showing the disrupted *DLGAP4* CpG island (CpG 107) to be hypermethylated (individual CpGs: filled circles) in the somatic cells of all male and female carriers tested. CpG methylation at *DLGAP4* is absent in purified spermatozoa DNA from translocation carrier IV.9 but is re-established in his somatic cells. (**F**) The undisrupted *DLGAP4* CpG island (CpG 107) is hypomethylated (individual CpGs: hollow circles) in all carriers. *DLGAP4* CpG island is bi-allelically hypomethylated in all related (IV.6 and V.6) and unrelated phenotypically normal controls (Controls 1 and 2).

Next, we asked whether this translocation-induced perturbed state of DNA hypermethylation at the truncated *DLGAP4* CpG island was maintained in germ cells of the translocation carriers. For this, we purified spermatozoa cells from two translocation carrier males (IV.4 and IV.9) (Fig. 1D) and carried out bisulfite allelic-sequencing using primers specific for the truncated or undisrupted *DLGAP4* breakpoint regions (Supplementary Material, Table S1). Spermatozoa purity was established prior to bisulfite allelic-sequencing (Supplementary Material, Fig. S2). Intriguingly, we found an erasure of this monoallelic hypermethylation, at the disrupted *DLGAP4* CpG island, in purified spermatozoa of the two tested male translocation carriers (IV.4, IV.9) (Fig. 2E and F). Thus, the monoallelic hypermethylation at the truncated *DLGAP4* CpG island may possibly be re-established *de novo* after each fertilization event (18–21) in embryos having the translocation chromosomes. These observations are in agreement with current models of epigenetic transmission (21–24). Since we found allele-specific changes in 5-mC at the disrupted *DLGAP4* CpG island, we hypothesized a possible change in the distribution of 5-hmC (25) at this locus. However, we did not find any significant differences in the distribution of 5-hmC at the breakpoint or across the *DLGAP4* locus (Supplementary Material, Fig. S3).

Enrichment of the histone variant H2A.Z at the undisrupted *DLGAP4* CpG Island is translocation-dependent

The *DLGAP4* locus, disrupted by the translocation, is distributed with the silencing histone H3K27me3 (histone 3 trimethylated at lysine 27) in a range of normal somatic cell types (26). However, the silencing histone H3K27me3 is replaced by the active histone H3K4me3 (histone 3 trimethylated at lysine 4) at this same *DLGAP4* locus in post-mortem human brain tissue (27), suggesting a change in local chromatin conformation specifically in the brain.

Thus, we tested for translocation-dependent changes in chromatin organization using chromatin immunoprecipitation (ChIP) followed by high-throughput sequencing (ChIP-Seq) and purified chromatin fractions from the lymphoblastoid cell lines (LCLs) of translocation carriers using antibodies for H2A.Z, H3K4me3 and H3K27me3 (Supplementary Material, Table S2). We re-confirmed the presence of monoallelic DNA hypermethylation at the disrupted *DLGAP4* CpG island in these carrier LCLs and found that it was maintained (Supplementary Material, Fig. S4A). Additionally genome-wide analysis of our ChIP-Seq data also showed an established distribution of histones relative to the transcription start sites at gene loci in the genome (Supplementary Material, Fig. S5).

Interestingly, we found a significant enrichment of the conserved histone variant H2A.Z at the *DLGAP4* CpG island, which was not present in any of the controls tested here (Fig. 3A and Supplementary Material Fig. S6A) or in published controls reported elsewhere (26,28,29), suggesting a translocation-dependent recruitment of this histone variant. Next , we investigated the allele specificity of the conserved histone variant H2A.Z at the *DLGAP4* locus using ChIP, followed by bisulfite allelic sequencing in two carriers and found unexpectedly that the H2A.Z antibody enriched specifically for the undisrupted and hypo/unmethylated *DLGAP4* allele (chr20) in translocation carriers (Fig. 3B and C).

Similarly, there was an enrichment of H3K4me3 across the *DLGAP4* locus shifting the chromatin state to an open conformation, which was not present in controls (Supplementary Material, Fig. S6A). In contrast however, we observed no differences in H3K27me3 distribution at the *DLGAP4* locus in translocation carriers compared with controls (Supplementary Material, Fig. S6A), nor did we identify any significant changes in the chromatin organization at the disrupted 8p12 locus in carriers compared with that in controls (Supplementary Material, Fig. S6B).

Delayed replication timing of the disrupted *DLGAP4* locus in *S-phase*

Acquired chromosomal rearrangements in human cancers have been associated with delayed mitotic condensation, delayed replication timing and mitotic instability (30). To gain insight into possible replication timing changes mediated by the t(8;20) translocation, we developed a replication timing analysis assay by using DNA fluorescence *in situ* hybridization (DNA *FISH*) on 5-bromo-2′-deoxyuridine (BrdU)-incorporated nuclei (31,32) of unsynchronized LCLs from two translocation carriers and two normal controls. We used probes adjacent to the breakpoints at 8p12 and 20q11.23 (Fig. 3D and E). We found that the disrupted *DLGAP4* allele located on the der8 (BAC probe CTD-2182L9) and der20 (BAC probe CTD-2301L1) chromosomes replicated asynchronously and mainly in late *S-phase* in BrdU positive nuclei (Fig. 3F–H). This contrasted strongly with the undisrupted *DLGAP4* allele on chr20 (Fig. 3F–I) and the 8p12 locus on the normal chr8 and der20 (Fig. 3J and K), all of which remained early replicating in *S-phase* as observed in the control cells (Fig. 3I and K). The delay in replication timing of the disrupted *DLGAP4* locus on der8 was statistically significant (Fig. 3L and M).

Epigenetic remodelling induced by the t(8;20) translocation perturbs expression of *DLGAP4*

Data presented thus far indicate that monoallelic epigenetic modifications may deregulate expression of *DLGAP4* in t(8;20) carrier cells. We investigated whether these epigenetic perturbations functionally altered the expression of *DLGAP4* mRNAs and DLGAP4 protein levels in t(8;20) carrier cells.

At least three splice variants of *DLGAP4* (mRNA isoforms a, b and c) have been annotated (RefSeq database) and that are transcribed from the sense strand. We found that *DLGAP4* mRNA isoform a, physically disrupted by the t(8;20) translocation, was expressed exclusively in the human brain (Fig. 4A and B). Thus, we were unable to assess changes in the expression of this isoform in translocation carriers, because of the unavailability of brain tissue from carriers. *DLGAP4* mRNA isoforms b and c, however, showed tissue-wide expression in a high-throughput RNA-Seq control human tissue-panel (Fig. 4A). We chose to quantify the expression of *DLGAP4* mRNA isoform b, after confirming that it was widely expressed in most human tissues including the brain using quantitative real-time PCR (Fig. 4C). We found *DLGAP4* mRNA isoform b to have slightly increased expression in cell lines from translocation carriers compared with that from control cell lines (Fig. 4D).

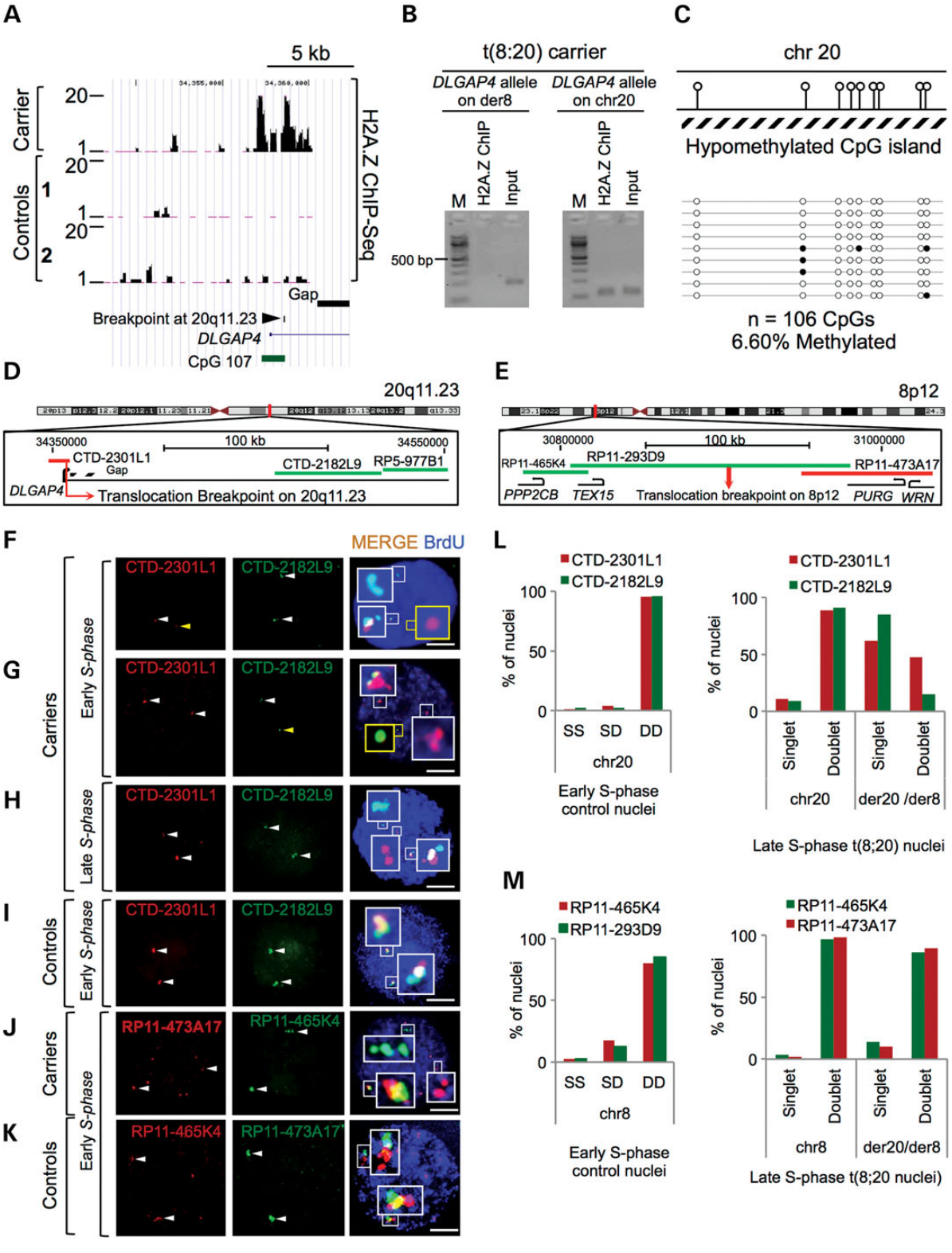

Figure 3. Monoallelic chromatin modifications at *DLGAP4* induced by the t(8;20) translocation. (**A**) The UCSC genome browser view of ChIP-Seq analysis showing H2A.Z enrichment (H2A.Z ChIP-Seq) at the *DLGAP4* locus. (**B** and **C**) H2A.Z ChIP followed by bisulfite allelic sequencing at *DLGAP4*. The H2A.Z antibody enriches for hypomethylated CpGs (individual CpGs: hollow circles) at the undisrupted chr20 homologue of *DLGAP4*. (**D** and **E**) Maps of loci showing biotin (green) and digoxigenin (red) labeled probes used for DNA *FISH* and replication timing analysis. (**F** and **G**) Representative images of BrdU (blue) positive early S-phase replicating nuclei showing the disrupted *DLGAP4* allele to replicate asynchronously (singlet's, yellow arrows). The undisrupted *DLGAP4* allele (doublets, white arrows) replicates in early S-phase. Scale bars 10 μm. (**H**) Representative images showing the disrupted *DLGAP4* allele to have replicated in BrdU (blue) positive late S-phase nuclei (doublets, white arrows). Scale bars 10 μm. (**I**) Both *DLGAP4* homologues (doublets, white arrows 2DD) replicate in early S-phase in multiple

Next, to evaluate monoallelic changes in expression of *DLGAP4* isoform b due to the allele-specific changes in DNA methylation, we constructed mouse-human E2 cell hybrids containing only a single derivative (der8 or der20) or normal (chr20 or chr8) human chromosome derived from translocation carriers (Supplementary Material, Fig. S4B and D) (33). We confirmed that monoallelic hypermethylation at the disrupted *DLGAP4* CpG island on the der8 allele was retained in these mouse-human E2 cell hybrids (Supplementary Material, Fig. S4A). Strikingly, we found that the *DLGAP4* mRNA isoform b had increased expression in mouse-human E2 cell hybrids containing the derivative 8 chromosome, compared with its expression in cells with an undisrupted chromosome 20 (Fig. 4E, $P < 0.01$).

Furthermore, we noted that *DLGAP4* mRNA isoform a was specifically expressed in the external granular layer cells of fetal cerebellum (21 weeks post gestation) and in Purkinje neurons of adult human brains (Fig. 4F). We also found that *DLGAP4* mRNA isoform b was similarly expressed in Purkinje neurons of the adult human brain (Fig. 4G). In agreement with our *DLGAP4* mRNA monoallelic expression analysis, protein expression analyses revealed increased levels of the DLGAP4 protein in the carrier LCLs compared with that in controls (Fig. 4H). We also found that the DLGAP4 protein was highly expressed in Purkinje neurons and the external granular layer cells of human fetal brain (21 weeks post gestation), which was similar to the expression of *DLGAP4* mRNAs. These data underscore the functional importance of DLGAP4 in neurons of the human cerebellum.

t(8;20) translocation disrupts bi-directionally expressed novel ncRNAs at *DLGAP4*

Since we found *DLGAP4* mRNA isoform a to be disrupted by the t(8;20) translocation and to be specifically expressed in human brain tissue, we set out to annotate non-coding elements within its promoter region that could potentially regulate its expression in the brain. Indeed, the expression of brain-specific genes is associated with the regulatory effects of different types of functional elements including ncRNAs that act in *cis* or *trans* and which are transcribed from within the gene's promoter region (34,35). Initially, we carried out RNAz predictions (36) and identified a novel candidate ncRNA (386 bp) at position chr20:34358650–34359035 (NCBI 36/hg18 genome-assembly), which was disrupted by the t(8;20) breakpoint (Fig. 5A). This ncRNA is transcribed from within the intron of the *DLGAP4* promoter, downstream of the first untranslated exon of mRNA isoform a (*DLGAP4* exon 1).

Using anti-sense oligos listed in Supplementary Material, Table S3 together with RNA *FISH*, we confirmed that *DLGAP4* mRNA isoform a was expressed significantly in Purkinje neurons and only from the sense strand in the adult human cerebellum (Fig. 5B). Interestingly, we found that the ncRNA at *DLGAP4* was expressed from both the sense and anti-sense strands in the adult human cerebellum (Fig. 5C and D). The striking bi-directional and complementary expression pattern of this ncRNA at *DLGAP4*, which was evaluated using sense and anti-sense oligos, was also present in the adult mouse cerebellum (Fig. 5E), suggesting a conserved role and its possible involvement in the regulation of *DLGAP4* expression in the brain. We quantified the expression of this candidate ncRNA at *DLGAP4* and found that its expression level was high in the human brain, with reduced levels in most of the other tissues tested (Fig. 5F and Supplementary Material Fig. S7). Correspondingly, the ncRNA at *DLGAP4* was expressed at slightly higher levels in the LCLs of translocation carriers compared with that of controls, and in mouse-human E2 cell hybrids retaining the der8 homologue (Fig. 5G and data not shown). The complete size of this ncRNA could not be determined using northern blot analysis and radioactively labelled probes (data not shown). This could be due to the small size (<800 bp) of the probes used, low expression levels of the ncRNA (37) or other challenges associated with the northern blot technique (38).

DISCUSSION

The present study provides new evidence and mechanistic insight linking epigenetic and genetic factors with the deregulation of a truncated CpG island, thereby altering expression of *DLGAP4*, a new candidate gene involved in the development of mild, early-onset non-progressive cerebellar ataxia.

The significant LOD score of $Z = 5.12$ ($\theta = 0.0$) and the absence of genes at the other breakpoint suggest *DLGAP4* to be a strong candidate for early-onset, non-progressive, mild cerebellar ataxia (6). With respect to function, DLGAP4 is also a very attractive candidate since the DLGAP4 protein is a member of the Membrane Associated Guanylate Kinase (MAGUK) family, which contains five similar proteins, i.e. DLGAP 1–5. DLGAP4 is highly expressed in the post-synaptic density (PSD), where it is possibly associated with the clustering of PSD proteins like PSD95 and SHANK family members via their PDZ domains (15,39,40). DLGAP4 also interacts with signalling molecules involved in the N-methyl-D-aspartate receptor signalling pathway in postsynaptic neurons (41), and has previously been reported to be an intrinsic component of the PSD95 core complex (39). DLGAP4 is expressed only in the thalamostriatal synapses in the striatum but not in the oculostriatal synapses where DLGAP3 is expressed (16). This finding of molecular specificity in post-synaptic scaffold attributes a specific function to DLGAP4 and the other members of the DLGAP/SAPAP family. Thalamostriatal synapses, where Dlgap4 is expressed, are implicated in movement disorders. They are significantly degenerated in the brains of patients with Parkinson's disease. Deep stimulation of these neurons helps to ease the motor symptoms in Tourette syndrome and other movement disorders (42). The disruption of gene products that are highly expressed in Purkinje neurons is also associated with movement disorders including cerebellar ataxia (43) and is compatible with

controls. BrdU stained nuclei are show in blue. Scale bars 10 μm. (**J** and **K**) Both 8p12 loci on translocation chromosomes [der8 and der20 (2DD, white arrows)] and undisrupted chromosome [chr8 (2DD, white arrows)] remain early replicating in translocation carriers, similar to that in controls. Scale bars 10 μm. BrdU stained nuclei are show in blue. Scale bars 10 μm. (**L**) Statistical analyses show a higher percentage of delayed replicating *DLGAP4* allele (singlet, S) in only the der8 homologue of carriers (CTD-2182L9 green bars). 100 BrDU positive nuclei were quantified in each case. Replicated loci are annotated as doublets (DD). (**M**) Statistical analyses show that 8p12 remains early replicating in carriers similar to that in controls. 100 BrDU positive nuclei were quantified in each case. Unreplicated loci are annotated as singlets (S), whereas replicated loci are annotated as doublets (DD).

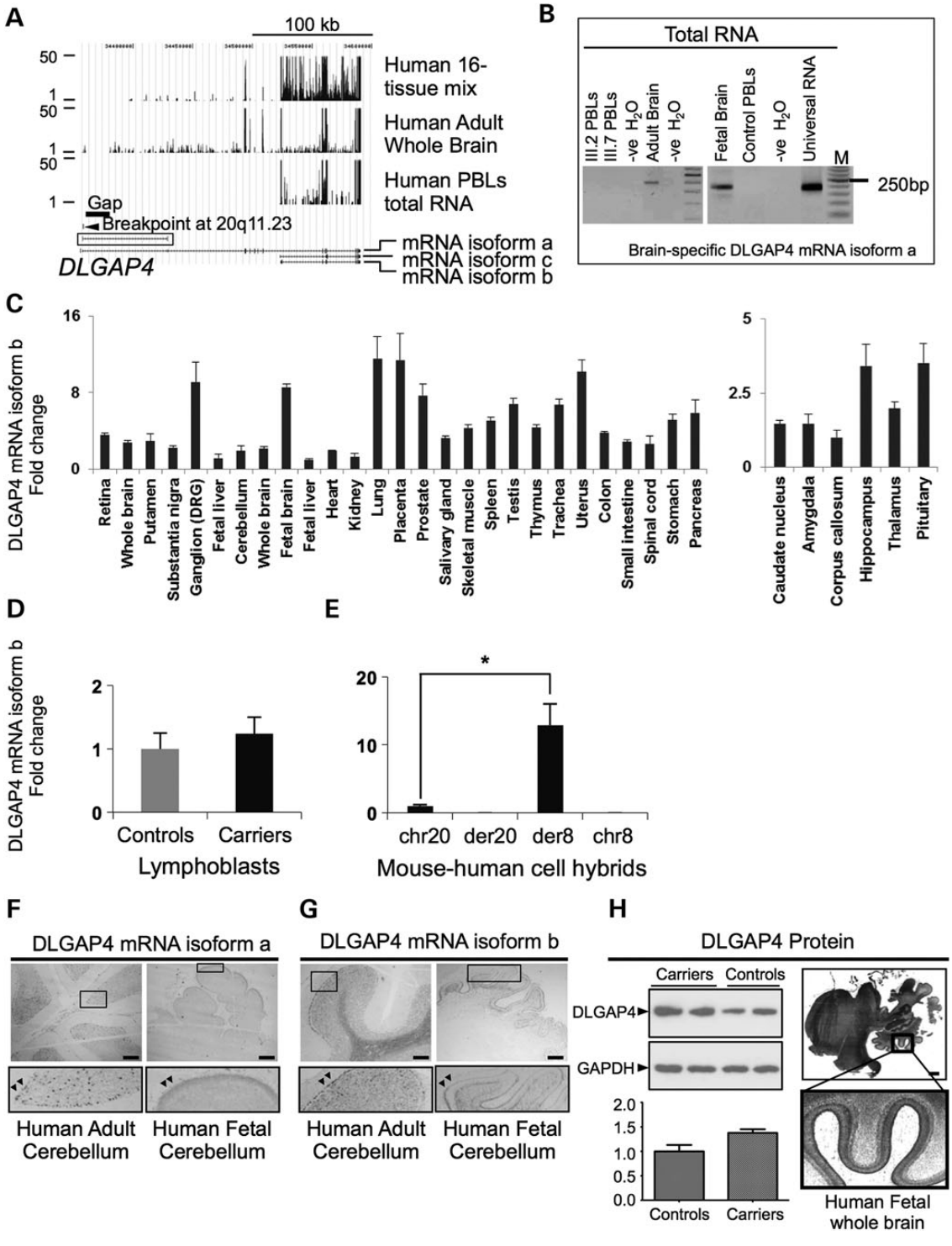

Figure 4. t(8;20) perturbs expression of *DLGAP4* gene products in translocation carriers. (**A**) The representative UCSC Genome Browser view illustrates the expression of *DLGAP4* mRNA isoforms a, b and c using high-throughput RNA-Seq. (**B**) Quantification of *DLGAP4* mRNA isoform a expression in carrier and control human tissues. **(C)** Quantification of the *DLGAP4* mRNA isoform b in a human multi-tissue panel. Error bars show the range. (**D** and **E**) Increased expression of *DLGAP4* mRNA isoform b in translocation carrier LCLs and higher monoallelic expression in hybrid cells having the translocated der8 allele. Error bars show the range. *Indicates $P < 0.01$. (**F** and **G**) *In situ* hybridizations showing expression of *DLGAP4* mRNA isoforms a and b (darkly stained regions) in Purkinje neurons in adult human cerebellum and external granular layer cells of fetal human cerebellum, respectively. Selected regions are shown at higher magnification in separate panels below. Scale bars 1 mm. (**H**) Western blots showing elevated expression of DLGAP4 (108 kDa) protein in translocation carrier LCLs compared with controls. Error bars show the range. Immunohistochemistry showing DLGAP4 protein expression in Purkinje neurons and external granular layer cells of control human fetal cerebellum (darkly stained regions). Selected regions are shown at higher magnification in a separate panel. Scale bars 1 mm.

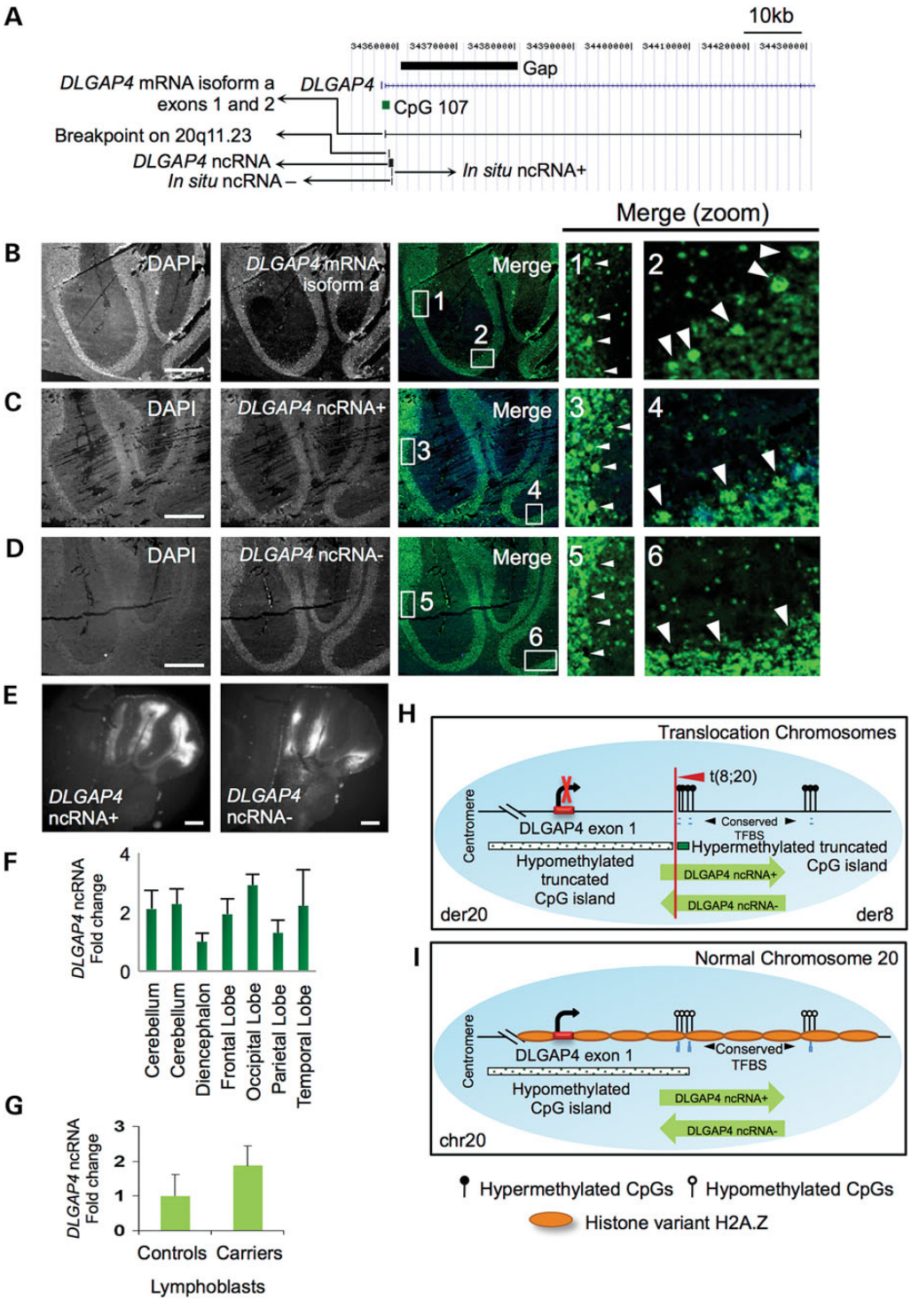

Figure 5. t(8;20) disrupts novel bi-directionally expressed ncRNAs at *DLGAP4*. (**A**) UCSC Genome Browser snapshot showing the breakpoint locus on 20q11.23 annotated with *DLGAP4* mRNA isoform a and novel bi-directional *DLGAP4* ncRNAs (ncRNA+ and ncRNA−). (**B**–**D**) *In situ* hybridizations showing the spatio-temporal expression of *DLGAP4* mRNA isoform a, *DLGAP4* ncRNA+ and ncRNA− in adult human cerebellum sections. Selected regions are shown at higher magnification in numbered boxes. White arrows show the regions of high expression. Note that *DLGAP4* mRNA isoform a and ncRNA+ are highly expressed in Purkinje neurons of the human cerebellum. The *DLGAP4* ncRNA− is more abundant in the molecular layer of the adult human cerebellum. *DLGAP4* mRNA (isoform a) appears to have an increased abundance in the cytoplasm of Purkinje cells, whereas *DLGAP4* ncRNA+ appears to be localized in the nucleus and the cytoplasm of these cells. Selected regions are shown at higher magnification in separate panels. Scale bars, 1 mm. (**E**) Bi-directional and complementary expression of Dlgap4 ncRNA+ and Dlgap4 ncRNA− in adult mouse cerebellum brain sections. Scale bars, 1 mm. (**F**) Quantification of *DLGAP4* candidate ncRNA expression in the total RNA from a human brain panel. Error bars show the range. (**G**) Slightly increased expression of *DLGAP4* ncRNA is identified in translocation carriers compared with controls. Error bars show the range. (**H** and **I**) Model showing ncRNAs at *DLGAP4*, relative to monoallelic CpG methylation, H2A.Z enrichment and *DLGAP4* mRNA isoform a expression at the disrupted (der20/der8) and undisrupted (chr20) *DLGAP4* homologues of translocation carriers. TFBS (HMR conserved TFBS UCSC track, hg18) includes binding sites for RP58 and USF1.

our finding that *DLGAP4* gene products (mRNAs and protein) were abundant in human Purkinje neurons. Additionally, single nucleotide polymorphisms within the 20q11.21–q13.12 locus and comprising the *DLGAP4* gene have been linked with the development of early onset autism spectrum disorders (44,45). Moreover, altered methylation patterns have been found in three CpG islands within the *SHANK3* gene (coding for the SH3 and ankyrin domain containing protein, a known interaction partner of DLGAP4) (40), in post-mortem brain samples from autism spectrum disorder patients, which is accompanied with altered expression and alternative splicing of the *SHANK3* gene (22).

Taken together, our data link the monoallelic epigenetic changes (Fig. 5H and I) induced by a chromosome translocation co-segregating with a specific cerebellar ataxia phenotype to deregulate *DLGAP4*, a strong disease-associated candidate gene. The data suggest that these epigenetic changes including the transmitted changes in DNA methylation at the disrupted CpG island deregulate *DLGAP4* expression in somatic cells of the affected individuals. This establishes DLGAP4 as a strong candidate gene for the associated cerebellar ataxia phenotype. It is conceivable that the epigenetic and gene expression changes identified here may be representing the deregulated *DLGAP4* in the brains of affected carriers having the t(8;20) translocation.

Our finding of transmission of altered, locus-specific DNA hypermethylation which is induced by an inherited constitutional translocation and associated with a neurodevelopmental disorder is reminiscent of that observed in cancer (23). We speculate that other chromosomal aberrations, which disrupt specific regulatory regions of the nuclear genome in diseases other than cancers, may also be associated with monoallelic epigenetic perturbations that affect expression of the disrupted loci.

Previous studies have provided conflicting results on the relationship between replication timing and the transcriptional state of a particular locus, including imprinted regions (32). Our findings of an inverse correlation between gene expression and replication timing at the disrupted *DLGAP4* locus suggest a more complex association. Indeed, increased monoallelic expression of *DLGAP4* mRNA isoform b from the translocated locus may be a result of the region coming into close proximity with certain *cis*-acting elements on 8p12, which could potentially regulate expression from the translocated locus, as previously reported (46). If so, this suggests a functional link between the altered replication timing and the gene loci lying adjacent to the breakpoint with the correct direction of transcription.

Enrichment of H2A.Z at the undisrupted and hypomethylated allele of the *DLGAP4* CpG island on chr20 is concordant for its antagonistic relationship with DNA hypermethylation that we identified on the truncated *DLGAP4* allele on der8. H2A.Z exchange at nucleosomes is associated with the regulation of gene expression, which prevents the spread of heterochromatin and/or maintains the epigenetic memory of a gene's previous transcriptional state (47–49).

A probable scenario is that the re-organization of histones in the promoter region of *DLGAP4* mRNA isoform a may be catalyzed by the activity of *DLGAP4* ncRNA(s) identified in this study and transcribed from within the disrupted *DLGAP4* intron (35,50). We found these *DLGAP4* ncRNAs (ncRNA+ and ncRNA-) to be bi-directionally expressed in the adult human and mouse cerebellum. It is conceivable that these ncRNAs may facilitate the specific expression of *DLGAP4* mRNA isoform a in Purkinje neurons of the brain by recruiting chromatin-modifying factors and/or transcription factors (51).

In summary, our results provide a potential breakthrough into the complex causes of congenital neurodevelopmental disorders. Additionally, we identify a new mechanism linked with cerebellar ataxia wherein truncation of the CG-rich *DLGAP4* promoter region induces monoallelic epigenetic remodelling of the locus associated with the perturbed expression of its gene products. Furthermore, we establish *DLGAP4* as a new candidate gene associated with early-onset non-progressive mild, cerebellar ataxia.

MATERIALS AND METHODS

Cell culture

LCLs were established as published elsewhere (52) using PBLs from carriers (III.2, III.7, IV.1, IV.2, IV.4, IV.9, V.1 and V.7), unrelated normal controls (1, 2, 3 and 4) and related normal controls (IV.6 and V.6). Somatic cell hybrids were constructed from translocation carrier LCLs (III.2 and III.7), using mouse E2 cells as previously described (33).

Genomic DNA isolation

Somatic cell and/or purified spermatozoa DNA was isolated using the FlexiGene DNA Kit according to the manufacturer's instructions (Qiagen). Spermatozoa were purified from a semen sample of a male translocation carrier, using the SilSelect Plus gradient system according to the manufacturer's instructions (FertiPro). Isolated spermatozoa DNA was repurified using the Gentra Puregene kit (Qiagen).

Mapping of translocation breakpoints and linkage analysis

Breakpoints on 8p12 and 20q11.23 were mapped using DNA *FISH* within BAC clones RP11-293D9 and CTD-2301L1 in carriers. Southern blot analysis was performed to characterize breakpoints as previously published (53). Briefly, hybridization of a PCR product (bases 89 335–90 118 of BAC clone RP11-293D9) on 8p12 of translocation carrier DNA cut with different restriction enzymes showed aberrant bands specific for the breakpoint region. An 800 bp *Mbo*I junction fragment was cloned using adaptor ligated PCR. Nested PCRs using chromosome 8p12 specific primers and adaptor primers yielded the expected product of 450 bp, confirmed using BLAST. Breakpoints were amplified in all carriers using primers listed in Supplementary Material, Table S1. Two-point LOD score was calculated using LIPED where theta is equal to 0 (as a dominant inheritance) with allele frequencies of 0.001 for the disease and translocation breakpoint as published elsewhere (54).

Methylated (5mC) and hydroxymethylated (5hmC) DNA immunoprecipitation (IP)

Two to four micrograms of isolated PBL genomic DNA from carriers or phenotypically normal controls was either nebulized (Invitrogen) or sonicated, followed by purification using the QIAquick purification kit and columns (Qiagen) as previously

done (14). IP of hypermethylated or hydroxymethylated fragmented DNA was performed using either his-MBD2b antibody (0.1 μg/μl) with the MethylCollector kit (Active Motif) or a 5 hmC antibody with the hMeDIP kit (Diagenode) according to the manufacturer's instructions. A further clean up step was performed after 5-mC IP using the MinElute PCR purification kit (Qiagen).

Methylation sensitive restriction enzyme digestion (MRE)

Restriction enzyme (RE) digestion of PBL DNA (2 μg) from carriers or controls was performed using methylation sensitive *Hpa*II according to the manufacturer's instructions (New England Biolabs). Digested DNA was size selected using 2% agarose TBE gel electrophoresis. One hundred and fifty to three hundred base pair regions were excised and purified using the Qiagen Gel extraction kit according to the manufacturer's instructions.

Chromatin immunoprecipitation (ChIP)

ChIP was performed with the ChIP-IT Express kit (Active Motif) essentially as described by the manufacturer or as published previously (55) on chromatin isolated from LCLs of the indexed carrier and her sister (III.2 and III.7) using histone antibodies listed in Supplementary Material, Table S2. ChIP-Seq using antibodies against H2A.Z were performed using LCLs from the same controls (1 and 2) as done for methylation analysis.

High-throughput sequencing of RNA (RNA-Seq)

High-throughput RNA-Seq Body Map 2.0 sequence data archived at the European Nucleotide Archive (ENA) under accession number ERP000546 was obtained and used for expression analysis of human tissues as described elsewhere (56).

Library preparation for high-throughput Illumina sequencing

Library generation of immunoprecipitated chromatin, un/hydroxy/hypermethylated DNA for Illumina sequencing was performed using a manufacturer recommended protocol and sequenced on a Genome Analyzer II (Illumina). ENCODE raw sequenced reads for H2A.Z and H3K4me3 ChIP on GM12878, control LCLs were also obtained from the genome browser at UCSC (57). Sequenced reads from all experiments were aligned back to the hg18 assembly using Bowtie (58). Two mismatches within the seed sequence of each unique aligned read were used as cut-offs. ChIP-Seq, MBD-Seq, MRE-Seq and hMeDIP-Seq data were analysed using Cisgenome, a false discovery rate of <0.01 (59) and visualized using the UCSC or Cisgenome genome browsers. ChIP-Seq and hMeDIP-Seq data were analysed using two sample analyses with histone H3 or IgG as negative controls. Genome-wide comparisons of MBD-Seq and ChIP-Seq data were performed using the R-environment for statistical computing (www.r-project.org) (60).

Bisulfite allelic sequencing

Bisulfite conversion of gDNA was performed using the Methylation-Gold kit (Zymo Research) according to the manufacturer's instructions, followed by methylation-specific PCR (MSP-PCR) using allele-specific primers (Supplementary Material, Table S1). PCR products were cloned using the TOPO-TA vector, one shot Mach1−T1 competent cells (Invitrogen), incubated at 37°C for 8−12 h using ampicillin selection followed by PCR and Sanger sequencing (ABI 3130XL) of 10−20 picked colonies. Sequenced reads were analyzed using BiQ Analyser (61). Bisulfite allelic sequencing was performed similarly following ChIP using H2A.Z and chromatin from LCLs and was performed with *DLGAP4* allele-specific primers and eluted DNA.

Expression analysis

Complementary DNA (cDNA) was prepared using Superscript II Reverse Transcriptase (Invitrogen). Total RNA was extracted with TRIzol from carrier cells, control cells or purchased (human fetal brain, human adult total brain, total RNA from various human tissues: Clontech and universal human reference RNA: Stratagene). QPCR was performed in triplicates using cDNA from multiple samples using the light cycler FastStart DNA Masterplus SYBR green I (Roche) and run on an Opticon 2 thermocycler (Bio-Rad). qPCR data were normalized with a geometric mean normalization factor (geNorm calculation) (62) using housekeeping genes (Supplementary Material, Table S1). *COX4I1, GAPDH, ATP5A, ALAS1 PBGD* and *ATP6A* were used for calculating the normalization factor for expression data of *DLGAP4* isoform b in the human multi-tissue panel. *RPL13, GAPDH, G6PD, PBGD* and *ALAS1* were used for normalizing expression data of mouse-human cell hybrids. These expression data were further adjusted using percentages of retained single human chromosomes in mouse-human hybrid cells, using DNA *FISH* and 20q11.23 or 8p12 biotin/digoxigenin labelled probes. *GAPDH, G6PD, ALAS1* and *B2M* were used for normalizing expression data from LCLs. Normalization of human brain panel RNA (BioCat) data was performed with *ATP5A1, COX4I1, ATP6A, ALAS1, B2M, ATP8A, PBGD, G6PD, HPRT* and *GAPDH*.

Northern blot analysis

Northern blot analysis was carried out using purchased total human cerebellum RNA of a normal control (Cat # 4099, Capital Biosciences) and total brain RNA (Clontech). After PCR, amplified products were purified using the QIAquick purification kit and columns (Qiagen). Northern blotting was carried out using methods published elsewhere (63,64). Purified PCR products were either body-labeled by the random primer method and [γ-^{32}P] ATP or end-labeled with T4 PNK and [γ-^{32}P] ATP (specific activity >3000 Ci/mmol, PerkinElmer).

In situ hybridizations and immunohistochemistry

In situ hybridizations were performed using *FITC* or peroxidase-conjugated oligos (Supplementary Material, Table S3) and control adult/fetal human/mouse brain or human cerebellum sections (Capital Biosciences) as previously published (65). Immunohistochemistry on adult or fetal human brain sections was performed using standard protocols. Human fetal brain sections used in this study were obtained from a midgestation fetus (21

weeks post gestation). Signals were analysed using an MVX10 microscope, F-View black/white, Colour-View cameras and Cell^P software (Olympus).

Western blots

Protein extracts were prepared from LCLs whole cell lysates using CelLytic M cell lysis solution and Protein inhibitor cocktail (Sigma). Western blots were prepared in duplicates, using equivalent protein concentrations and Novex NuPAGE Tris-Acetate gel electrophoresis (Invitrogen). Primary antibodies were incubated with the membrane overnight at 4°C in 5% skimmed milk and detected using secondary antibodies (Supplementary Material, Table S2). ECL (Amersham) was used for signal detection.

DNA *FISH* and replication timing analysis

Replication timing analysis was performed using DNA *FISH* and BrdU pulse labelled exponentially growing carrier or control LCLs (31,32). Cells were arrested at 5 or 9 h post BrdU incorporation, indicative of early or late replication timing respectively (32). DNA *FISH* was performed using biotin/digoxigenin labelled probes (purchased from the BACPAC resource or Sanger Center, UK) for the 20q11.23 or 8p12 loci. Following detection and mounting of slides with antifade Prolong GOLD without DAPI (Invitrogen), signals were identified in BrdU incorporated nuclei as replicated doublets (D), or un-replicated singlet's (S), using a DMRXA epifluorescence microscope, DFC340 FX camera and CW4000 Karyo software (Leica).

Data access

High throughput data have been archived at GEO under accession number GSE31204 (http://www.ncbi.nlm.nih.gov/geo/query/acc.cgi?acc=GSE31204).

SUPPLEMENTARY MATERIAL

Supplementary Material is available at *HMG* online.

ACKNOWLEDGEMENTS

The authors thank all contributing past and present technical staff of WJC and MPIMG. We thank Mrs Karen Friis Henriksen for her immense help throughout the project, Ms Zahra El-Schich for technical assistance, Prof Morten Møller for brain sections and initial ISH analysis, Prof Henrik Nielsen and Dr Knud Josefsen for assistance with northern blot analysis. Finally, we thank the members of the very cooperative cerebellar ataxia family mentioned in the study.

Conflicts of Interest statement. None declared.

FUNDING

This study was supported by the Lundbeck Foundation (A.S., N.T.), the Danish National Research Foundation (N.T.), the Danish National Research Council and the Danish Ministry of Science, Technology and Innovation, and the National Genome Research Network (NGFN). S.M. was a Marie Curie Early Stage Research Fellow funded by the Marie Curie RTN *'Chromatin Plasticity'* (*EU FP6*) grant (MRTN – CT-2006-035733) awarded to A.S. Funding to pay the Open Access publication charges for this article was provided by the University of Copenhagen, Denmark.

REFERENCES

1. Borrelli, E., Nestler, E.J., Allis, C.D. and Sassone-Corsi, P. (2008) Decoding the epigenetic language of neuronal plasticity. *Neuron*, **60**, 961–974.
2. Kilpinen, H., Waszak, S.M., Gschwind, A.R., Raghav, S.K., Witwicki, R.M., Orioli, A., Migliavacca, E., Wiederkehr, M., Gutierrez-Arcelus, M., Panousis, N.I. *et al.* (2013) Coordinated effects of sequence variation on DNA binding, chromatin structure, and transcription. *Science*, **342**, 744–747.
3. McVicker, G., van de Geijn, B., Degner, J.F., Cain, C.E., Banovich, N.E., Raj, A., Lewellen, N., Myrthil, M., Gilad, Y. and Pritchard, J.K. (2013) Identification of genetic variants that affect histone modifications in human cells. *Science*, **342**, 747–749.
4. Kasowski, M., Kyriazopoulou-Panagiotopoulou, S., Grubert, F., Zaugg, J.B., Kundaje, A., Liu, Y., Boyle, A.P., Zhang, Q.C., Zakharia, F., Spacek, D.V. *et al.* (2013) Extensive variation in chromatin states across humans. *Science*, **342**, 750–752.
5. Tommerup, N., Schempp, W., Meinecke, P., Pedersen, S., Bolund, L., Brandt, C., Goodpasture, C., Guldberg, P., Held, K.R., Reinwein, H. *et al.* (1993) Assignment of an autosomal sex reversal locus (SRA1) and campomelic dysplasia (CMPD1) to 17q24.3-q25.1. *Nat. Genet.*, **4**, 170–174.
6. Hertz, J.M., Sivertsen, B., Silahtaroglu, A., Bugge, M., Kalscheuer, V., Weber, A., Wirth, J., Ropers, H.H., Tommerup, N. and Tumer, Z. (2004) Early onset, non-progressive, mild cerebellar ataxia co-segregating with a familial balanced translocation t(8;20)(p22;q13). *J. Med. Genet.*, **41**, e25.
7. Bugge, M., Bruun-Petersen, G., Brøndum-Nielsen, K., Friedrich, U., Hansen, J., Jensen, G., Jensen, P.K.A., Kristoffersson, U., Lundsteen, C., Niebuhr, E. *et al.* (2000) Disease associated balanced chromosome rearrangements: a resource for large scale genotype-phenotype delineation in man. *J. Med. Genet.*, **37**, 858–865.
8. Mossman, J., Blunt, S., Stephens, R., Jones, E.E. and Pembrey, M. (1983) Hunter's disease in a girl: association with X:5 chromosomal translocation disrupting the Hunter gene. *Arch. Dis. Child.*, **58**, 911–915.
9. Sharp, A., Robinson, D. and Jacobs, P. (2001) Absence of correlation between late-replication and spreading of X inactivation in an X;autosome translocation. *Hum. Genet.*, **109**, 295–302.
10. Cleary, M.A., van Raamsdonk, C.D., Levorse, J., Zheng, B., Bradley, A. and Tilghman, S.M. (2001) Disruption of an imprinted gene cluster by a targeted chromosomal translocation in mice. *Nat. Genet.*, **29**, 78–82.
11. Takizawa, T., Meaburn, K.J. and Misteli, T. (2008) The meaning of gene positioning. *Cell*, **135**, 9–13.
12. Tufarelli, C., Stanley, J.A.S., Garrick, D., Sharpe, J.A., Ayyub, H., Wood, W.G. and Higgs, D.R. (2003) Transcription of antisense RNA leading to gene silencing and methylation as a novel cause of human genetic disease. *Nat. Genet.*, **34**, 157–165.
13. Genesio, R., Melis, D., Gatto, S., Izzo, A., Ronga, V., Cappuccio, G., Lanzo, A., Andria, G., D'Esposito, M., Matarazzo, M.R. *et al.* (2011) Variegated silencing through epigenetic modifications of a large Xq region in a case of balanced X;2 translocation with Incontinentia Pigmenti-like phenotype. *Epigenetics*, **6**, 1242–1247.
14. Minocherhomji, S., Seemann, S., Mang, Y., El-Schich, Z., Bak, M., Hansen, C., Papadopoulos, N., Josefsen, K., Nielsen, H., Gorodkin, J. *et al.* (2012) Sequence and expression analysis of gaps in human chromosome 20. *Nucleic Acids Res.*, **40**, 6660–6672.
15. Kindler, S., Rehbein, M., Classen, B., Richter, D. and Böckers, T.M. (2004) Distinct spatiotemporal expression of SAPAP transcripts in the developing rat brain: a novel dendritically localized mRNA. *Brain Res. Mol. Brain Res.*, **126**, 14–21.
16. Wan, Y., Ade, K.K., Caffall, Z., Ilcim Ozlu, M., Eroglu, C., Feng, G. and Calakos, N. (2014) Circuit-selective striatal synaptic dysfunction in the Sapap3 knockout mouse model of obsessive-compulsive disorder. *Biol. Psychiatry*, **75**, 623–630.
17. Straussman, R., Nejman, D., Roberts, D., Steinfeld, I., Blum, B., Benvenisty, N., Simon, I., Yakhini, Z. and Cedar, H. (2009) Developmental

programming of CpG island methylation profiles in the human genome. *Nat. Struct. Mol. Biol.*, **16**, 564–571.
18. Morgan, H.D., Santos, F., Green, K., Dean, W. and Reik, W. (2005) Epigenetic reprogramming in mammals. *Hum. Mol. Genet.*, **14**, R47–R58.
19. Chan, T.L., Yuen, S.T., Kong, C.K., Chan, Y.W., Chan, A.S.Y., Ng, W.F., Tsui, W.Y., Lo, M.W.S., Tam, W.Y., Li, V.S.W. *et al.* (2006) Heritable germline epimutation of MSH2 in a family with hereditary nonpolyposis colorectal cancer. *Nat. Genet.*, **38**, 1178–1183.
20. Feng, S., Jacobsen, S.E. and Reik, W. (2010) Epigenetic reprogramming in plant and animal development. *Science*, **330**, 622–627.
21. Ligtenberg, M.J.L., Kuiper, R.P., Chan, T.L., Goossens, M., Hebeda, K.M., Voorendt, M., Lee, T.Y.H., Bodmer, D., Hoenselaar, E., Hendriks-Cornelissen, S.J.B. *et al.* (2009) Heritable somatic methylation and inactivation of MSH2 in families with Lynch syndrome due to deletion of the 3′ exons of TACSTD1. *Nat. Genet.*, **41**, 112–117.
22. Zhu, L., Wang, X., Li, X.-L., Towers, A., Cao, X., Wang, P., Bowman, R., Yang, H., Goldstein, J., Li, Y.-J. *et al.* (2014) Epigenetic dysregulation of SHANK3 in brain tissues from individuals with autism spectrum disorders. *Hum. Mol. Genet.*, **23**, 1563–1578.
23. Hitchins, M.P., Wong, J.J.L., Suthers, G., Suter, C.M., Martin, D.I.K., Hawkins, N.J. and Ward, R.L. (2007) Inheritance of a cancer-associated MLH1 germ-line epimutation. *N. Engl. J. Med.*, **356**, 697–705.
24. Suter, C.M., Martin, D.I.K. and Ward, R.L. (2004) Germline epimutation of MLH1 in individuals with multiple cancers. *Nat. Genet.*, **36**, 497–501.
25. Tahiliani, M., Koh, K.P., Shen, Y., Pastor, W.A., Bandukwala, H., Brudno, Y., Agarwal, S., Iyer, L.M., Liu, D.R., Aravind, L. *et al.* (2009) Conversion of 5-methylcytosine to 5-hydroxymethylcytosine in mammalian DNA by MLL partner TET1. *Science*, **324**, 930–935.
26. Meissner, A., Mikkelsen, T.S., Gu, H., Wernig, M., Hanna, J., Sivachenko, A., Zhang, X., Bernstein, B.E., Nusbaum, C., Jaffe, D.B. *et al.* (2008) Genome-scale DNA methylation maps of pluripotent and differentiated cells. *Nature*, **454**, 766–770.
27. Maunakea, A.K., Nagarajan, R.P., Bilenky, M., Ballinger, T.J., D/'Souza, C., Fouse, S.D., Johnson, B.E., Hong, C., Nielsen, C., Zhao, Y. *et al.* (2010) Conserved role of intragenic DNA methylation in regulating alternative promoters. *Nature*, **466**, 253–257.
28. Barski, A., Cuddapah, S., Cui, K., Roh, T.Y., Schones, D.E., Wang, Z., Wei, G., Chepelev, I. and Zhao, K. (2007) High-resolution profiling of histone methylations in the human genome. *Cell*, **129**, 823–837.
29. Bernstein, B.E., Kamal, M., Lindblad-Toh, K., Bekiranov, S., Bailey, D.K., Huebert, D.J., McMahon, S., Karlsson, E.K., Kulbokas Iii, E.J., Gingeras, T.R. *et al.* (2005) Genomic maps and comparative analysis of histone modifications in human and mouse. *Cell*, **120**, 169–181.
30. Smith, L., Plug, A. and Thayer, M. (2001) Delayed replication timing leads to delayed mitotic chromosome condensation and chromosomal instability of chromosome translocations. *Proc. Natl Acad. Sci. USA*, **98**, 13300–13305.
31. Azuara, V. (2006) Profiling of DNA replication timing in unsynchronized cell populations. *Nat. Protocols*, **1**, 2171–2177.
32. Gribnau, J., Hochedlinger, K., Hata, K., Li, E. and Jaenisch, R. (2003) Asynchronous replication timing of imprinted loci is independent of DNA methylation, but consistent with differential subnuclear localization. *Genes Dev.*, **17**, 759–773.
33. Yan, H., Papadopoulos, N., Marra, G., Perrera, C., Jiricny, J., Boland, C.R., Lynch, H.T., Chadwick, R.B., de la Chapelle, A., Berg, K. *et al.* (2000) Conversion of diploidy to haploidy. *Nature*, **403**, 723–724.
34. Mercer, T.R., Dinger, M.E., Sunkin, S.M., Mehler, M.F. and Mattick, J.S. (2008) Specific expression of long noncoding RNAs in the mouse brain. *Proc. Natl Acad. Sci. USA*, **105**, 716–721.
35. Khalil, A.M., Guttman, M., Huarte, M., Garber, M., Raj, A., Rivea Morales, D., Thomas, K., Presser, A., Bernstein, B.E., van Oudenaarden, A. *et al.* (2009) Many human large intergenic noncoding RNAs associate with chromatin-modifying complexes and affect gene expression. *Proc. Natl Acad. Sci. USA*, **106**, 11667–11672.
36. Gruber, A.R., Neuböck, R., Hofacker, I.L. and Washietl, S. (2007) The RNAz web server: prediction of thermodynamically stable and evolutionarily conserved RNA structures. *Nucleic Acids Res.*, **35**, W335–W338.
37. Tani, H., Mizutani, R., Salam, K.A., Tano, K., Ijiri, K., Wakamatsu, A., Isogai, T., Suzuki, Y. and Akimitsu, N. (2012) Genome-wide determination of RNA stability reveals hundreds of short-lived non-coding transcripts in mammals. *Genome Res.*, **22**, 947–956.
38. Hüttenhofer, A. and Vogel, J. (2006) Experimental approaches to identify non-coding RNAs. *Nucleic Acids Res.*, **34**, 635–646.
39. Fernandez, E., Collins, M.O., Uren, R.T., Kopanitsa, M.V., Komiyama, N.H., Croning, M.D.R., Zografos, L., Armstrong, J.D., Choudhary, J.S. and Grant, S.G.N. (2009) Targeted tandem affinity purification of PSD-95 recovers core postsynaptic complexes and schizophrenia susceptibility proteins. *Mol. Syst. Biol.*, **5**, doi:10.1038/msb.2009.1027.
40. Sakai, Y., Shaw, C.A., Dawson, B.C., Dugas, D.V., Al-Mohtaseb, Z., Hill, D.E. and Zoghbi, H.Y. (2011) Protein interactome reveals converging molecular pathways among autism disorders. *Sci. Trans. Med.*, **3**, 86ra49.
41. Boeckers, T.M., Winter, C., Smalla, K.H., Kreutz, M.R., Bockmann, J., Seidenbecher, C., Garner, C.C. and Gundelfinger, E.D. (1999) Proline-rich synapse-associated proteins ProSAP1 and ProSAP2 interact with synaptic proteins of the SAPAP/GKAP family. *Biochem. Biophys. Res. Commun.*, **264**, 247–252.
42. Smith, Y., Galvan, A., Ellender, T.J., Doig, N., Villalba, R.M., Huerta-Ocampo, I., Wichmann, T. and Bolam, J.P. (2014) The thalamostriatal system in normal and diseased states. *Front. Syst. Neurosci.*, **8**, 5.
43. Jeste, D.V., Barban, L. and Parisi, J. (1984) Reduced Purkinje cell density in Huntington's disease. *Exp. Neurol.*, **85**, 78–86.
44. Allen-Brady, K., Miller, J., Matsunami, N., Stevens, J., Block, H., Farley, M., Krasny, L., Pingree, C., Lainhart, J., Leppert, M. *et al.* (2008) A high-density SNP genome-wide linkage scan in a large autism extended pedigree. *Mol. Psychiatry*, **14**, 590–600.
45. Schellenberg, G.D., Dawson, G., Sung, Y.J., Estes, A., Munson, J., Rosenthal, E., Rothstein, J., Flodman, P., Smith, M., Coon, H. *et al.* (2006) Evidence for multiple loci from a genome scan of autism kindreds. *Mol. Psychiatry*, **11**, 1049–1060.
46. Stoffregen, E.P., Donley, N., Stauffer, D., Smith, L. and Thayer, M.J. (2011) An autosomal locus that controls chromosome-wide replication timing and mono-allelic expression. *Hum. Mol. Genet.*, **20**, 2366–2378.
47. Brickner, D.G., Cajigas, I., Fondufe-Mittendorf, Y., Ahmed, S., Lee, P.-C., Widom, J. and Brickner, J.H. (2007) H2A.Z-mediated localization of genes at the nuclear periphery confers epigenetic memory of previous transcriptional state. *PLoS Biol.*, **5**, e81.
48. Valdes-Mora, F., Song, J.Z., Statham, A.L., Strbenac, D., Robinson, M.D., Nair, S.S., Patterson, K.I., Tremethick, D.J., Stirzaker, C. and Clark, S.J. (2012) Acetylation of H2A.Z is a key epigenetic modification associated with gene deregulation and epigenetic remodeling in cancer. *Genome Res.*, **22**, 307–321.
49. Xu, Y., Ayrapetov, M.K., Xu, C., Gursoy-Yuzugullu, O., Hu, Y. and Price, B.D. (2012) Histone H2A.Z controls a critical chromatin remodeling step required for DNA double-strand break repair. *Mol. Cell.*, **48**, 723–733.
50. Nagano, T., Mitchell, J.A., Sanz, L.A., Pauler, F.M., Ferguson-Smith, A.C., Feil, R. and Fraser, P. (2008) The Air noncoding RNA epigenetically silences transcription by targeting G9a to chromatin. *Science*, **322**, 1717–1720.
51. Orom, U.A., Derrien, T., Beringer, M., Gumireddy, K., Gardini, A., Bussotti, G., Lai, F., Zytnicki, M., Notredame, C., Huang, Q. *et al.* (2010) Long noncoding RNAs with enhancer-like function in human cells. *Cell*, **143**, 46–58.
52. Pattengale, P., Smith, R. and Gerber, P. (1973) Selective transformation of B lymphocytes by E.B. virus. *Lancet*, **302**, 93–94.
53. Gilling, M., Dullinger, J.S., Gesk, S., Metzke-Heidemann, S., Siebert, R., Meyer, T., Brondum-Nielsen, K., Tommerup, N., Ropers, H.-H., Tümer, Z. *et al.* (2006) Breakpoint cloning and haplotype analysis indicate a single origin of the common Inv(10)(p11.2q21.2) mutation among Northern Europeans. *Am. J. Hum. Genet.*, **78**, 878–883.
54. Ott, J. (1976) A computer program for linkage analysis of general human pedigrees. *Am. J. Hum. Genet.*, **28**, 528–529.
55. Pasini, D., Cloos, P.A.C., Walfridsson, J., Olsson, L., Bukowski, J.-P., Johansen, J.V., Bak, M., Tommerup, N., Rappsilber, J. and Helin, K. (2010) JARID2 regulates binding of the Polycomb repressive complex 2 to target genes in ES cells. *Nature*, **464**, 306–310.
56. Bradley, R.K., Merkin, J., Lambert, N.J. and Burge, C.B. (2012) Alternative splicing of RNA triplets is often regulated and accelerates proteome evolution. *PLoS Biol.*, **10**, e1001229.
57. Kent, W.J., Sugnet, C.W., Furey, T.S., Roskin, K.M., Pringle, T.H., Zahler, A.M. and Haussler, A.D. (2002) The human genome browser at UCSC. *Genome Res.*, **12**, 996–1006.
58. Langmead, B., Trapnell, C., Pop, M. and Salzberg, S. (2009) Ultrafast and memory-efficient alignment of short DNA sequences to the human genome. *Genome Biol.*, **10**, R25.

59. Ji, H., Jiang, H., Ma, W., Johnson, D.S., Myers, R.M. and Wong, W.H. (2008) An integrated software system for analyzing ChIP-chip and ChIP-seq data. *Nat. Biotech.*, **26**, 1293–1300.
60. Ihaka, R. and Gentleman, R. (1996) R: A Language for Data Analysis and Graphics. *J. Comput. Graph. Stat.*, **5**, 299–314.
61. Bock, C., Reither, S., Mikeska, T., Paulsen, M., Walter, J. and Lengauer, T. (2005) BiQ Analyzer: visualization and quality control for DNA methylation data from bisulfite sequencing. *Bioinformatics*, **21**, 4067–4068.
62. Vandesompele, J., De Preter, K., Pattyn, F., Poppe, B., Van Roy, N., De Paepe, A. and Speleman, F. (2002) Accurate normalization of real-time quantitative RT-PCR data by geometric averaging of multiple internal control genes. *Genome Biol.*, **3**, research0034.0031-research0034.0011.
63. Josefsen, K. and Nielsen, H. (2011) Northern blotting analysis. *Methods Mol. Biol.*, **703**, 87–105.
64. Andersen, K.L. and Nielsen, H. (2012) Experimental identification and analysis of macronuclear non-coding RNAs from the ciliate Tetrahymena thermophila. *Nucleic Acids Res.*, **40**, 1267–1281.
65. Silahtaroglu, A.N., Nolting, D., Dyrskjot, L., Berezikov, E., Moller, M., Tommerup, N. and Kauppinen, S. (2007) Detection of microRNAs in frozen tissue sections by fluorescence in situ hybridization using locked nucleic acid probes and tyramide signal amplification. *Nat. Protocols*, **2**, 2520–2528.